Gamow-Teller transitions from ^{11}Li and ^{12}Be

Toshio Suzuki*
Department of Physics, College of Humanities and Sciences, Nihon University Sakurajosui 3-25-40, Setagaya-ku, Tokyo 156, Japan

Takaharu Otsuka†
Department of Physics, Faculty of Science, University of Tokyo Hongo 7-3-1, Bunkyo-ku, Tokyo 113, Japan
and RIKEN, Hirosawa, Wako-shi, Saitama 351, Japan

(Received 9 December 1996)

The strength distributions of Gamow-Teller (GT) transitions from ^{11}Li and ^{12}Be are investigated. We study where the GT strengths of the transitions ^{11}Li $(3/2^-_{gs})\rightarrow{}^{11}$Be* $(1/2^-, 3/2^-, 5/2^-)$ are located incorporating quenching effects due to the Δ-hole contributions. The connection between the GT sum rule and effects of the halo structure of ^{11}Li are discussed. The narrowing of the gap between the p shell and the sd shell is found to change the structure of the GT strength distribution. The accuracy of the present calculation is tested for the GT decay from ^{9}Li. We further study the GT transition from ^{12}Be. The narrowing of the gap between the p and sd shells varies the transition strength to ^{12}Be (1^+_{gs}) as well as the GT distribution. The quenching of the transition strength $^{12}\text{Be}\rightarrow{}^{12}\text{B}$ (1^+_{gs}) suggests an enormous breaking of the neutron closed-shell structure of ^{12}Be. [S0556-2813(97)05308-9]

PACS number(s): 21.60.Cs, 23.40.−s, 27.20.+n

I. INTRODUCTION

Due to the recent developments of radioactive nuclear beams, much progress has been made on the studies of structures and reactions of neutron-rich unstable nuclei [1,2]. The ground state of ^{11}Li $(3/2^-)$ has a neutron halo due to the small two-neutron separation energy $S_{2n}=295\sim340$ keV [3,4]. The first excited state of ^{11}Be $(1/2^-, 0.32$ MeV) as well as the ground state $(1/2^+)$ have small neutron separation energies $S_n=183$ and 503 keV, respectively, and hence have a neutron halo, too. This has been confirmed for the ground state [5]. Level inversion of the lowest $1/2^-$ and $1/2^+$ states in ^{11}Be has been discussed [1,2] and explained, for example, by the variational shell model [6].

In our previous work [7], effects of the halo as well as those of the meson exchange currents were studied for the Gamow-Teller (GT) β transition ^{11}Li $(3/2^-_{gs})\rightarrow{}^{11}$Be $(1/2^-$, 0.32 MeV). These effects were found to be important to reduce transition matrix elements and to remedy deviations from the observed logft value of the GT transition. This GT transition has been shown [7] to play an indispensable role in identifying the structure of two-neutron halo of ^{11}Li. It is indicated that the two neutrons forming the halo are in the $p^2_{1/2}$ configuration only with 60–70 % probability, while they are in the sd shell with the remaining probability. The larger probability of the sd-shell configuration can be induced by the lowering of the effective single-particle energies of the sd shell in ^{11}Li. The GT transition, therefore, can be used to explore the decrease of the effective gap between the p and sd shells in such unstable nuclei.

Recently, additional measurements of the GT transition have been carried out at RIKEN [8] and ISOLDE [9], which indicate a stronger retardation of the transition than the previous measurement [10,11]. Here, we reinvestigate the structure of two-neutron halo in ^{11}Li by using the results of the two measurements. We will discuss the implications of these data for the probability of the $\nu p^2_{1/2}$ configuration in ^{11}Li. We, then, extend our study to GT transitions to higher states: ^{11}Li $(3/2^-)\rightarrow{}^{11}$Be* $(1/2^-, 3/2^-, 5/2^-)$. The present calculation will be shown to give a branching ratio to the $1/2^-$ state of ^{11}Be, as well as B (GT)'s to some states in reasonable agreement with experiments. We investigate effects of the narrowing of the gap between p and sd shells on the distribution of the GT strength.

We also study the GT transition from ^{12}Be. We investigate the effects of the narrowing of the gap between the p shell and sd shell on the transition strength to ^{12}B (1^+_{gs}) as well as the GT distribution.

In Sec. II, we discuss the GT transition from ^{11}Li $(3/2^-_{gs})$ to ^{11}Be $(1/2^-$, 0.32 MeV) as well as the GT strength distribution. The GT β decay from ^{9}Li is investigated in Sec. III to see the accuracy of the present calculation. In Sec. IV, we study the GT transition from ^{12}Be and investigate the structure of ^{12}Be.

II. GT TRANSITIONS IN ^{11}Li

A. GT transition to ^{11}Be $(1/2^-$, 0.32 MeV) and the structure of two-neutron halo in ^{11}Li

In our previous work [7], the GT transition ^{11}Li $(3/2^-_{gs})\rightarrow{}^{11}$Be $(1/2^-$, 0.32 MeV) was shown to play an important role in identifying the structure of two-neutron halo in ^{11}Li. Adjusting to the observed logft value of 5.58 ±0.03 due to Roeckl *et al.* [10] by lowering the single-particle energies of the sd shell, it was indicated that the probability of the $\nu p^2_{1/2}$ configuration in ^{11}Li is 60–70 %.

Recently, measurements of the GT transition were carried out at RIKEN [8] and ISOLDE [9], which suggest a stronger

*Electronic mail: suzuki@chs.nihon-u.ac.jp
†Electronic mail: otsuka@phys.s.u-tokyo.ac.jp

retardation of the transition than before: logft values of 5.67 ± 0.04 [8] and 5.73 ± 0.03 [9] were obtained, respectively.

Here, we reinvestigate the structure of two-neutron halo in ^{11}Li by using the results of the two recent measurements as well as the old one [10]. Note that throughout this study the $0s_{1/2}$ inner core is assumed. We take into account both the halo effects and the narrowing of the gap between p and sd shells. The halo reduces the overlap of radial wave functions of proton states ($\pi p_{1/2}$ and $\pi p_{3/2}$) with that of $\nu p_{1/2}$ state. Likewise, the overlap of the radial wave function of $\pi 1s_{1/2}$ with that of $\nu 1s_{1/2}$ state is reduced. Wave functions obtained from Woods-Saxon potentials fitted to the observed single-neutron separation energy (S_n) are used for the $\nu p_{1/2}$ and $\nu 1s_{1/2}$ single-particle halo wave functions. The value of S_n is taken to be 160 keV in ^{11}Li, which is half of the averaged two-neutron separation energy $S_{2n}=320$ keV. Here we use an average of the two experimental values, $S_{2n}=295$ keV [3] and $S_{2n}=340$ keV [4]. The resultant overlaps are $\langle \pi p | \nu p_{1/2} \rangle = 0.85$ and $\langle \pi 1s_{1/2} | \nu 1s_{1/2} \rangle = 0.625$, respectively. Note that the larger overlap for $p_{1/2}$ is due to the centrifugal barrier. Here, harmonic oscillator wave functions are used for the proton as well as for the $\nu p_{3/2}$ state because they are well bound. In our previous work [7], the neutron halo wave function was taken into account only for $\nu p_{1/2}$.

We change the probability of the $\nu p_{1/2}^2$ configuration by lowering the single-particle energy of $1s_{1/2}$ orbit and study the variation of the calculated logft values. Transition matrix elements are obtained in the p-sd shell-model configuration space, where excitations of up to two valence particles to the sd shell are allowed. A set of interactions, PSDMK2 [12], whose p-shell part corresponds to TBE (8-16) [13], is used. The interaction in the sd shell is the one obtained by Kuo [14], while the Millener-Kurath interaction [15] is used to excite particles from the p shell into the sd shell and to deexcite the other way. The contribution from the Δ_{33}-isobar exchange current is also taken into account [7]. As the overlap $\langle \pi p | \nu p_{1/2} \rangle = 0.85$ is not far from unity, effects of the halo on the two-body shell model matrix elements are expected to be rather small compared to the case of β-decay matrix elements, because of finite-range nature of the two-body interactions.

The calculated results are shown in Fig. 1 together with the three experimental logft values. Here, we change only the single-particle energy of the $1s_{1/2}$ orbit. The changes of the single-particle energy of the $1s_{1/2}$ orbit, $\Delta\epsilon_{1s_{1/2}}$, are denoted in the figures. The $1s_{1/2}$ neutron also forms a halo in addition to the $\nu p_{1/2}$ orbit in Fig. 1(a), while a harmonic oscillator wave function is taken for the $1s_{1/2}$ orbit in Fig. 1(b). Combining Figs. 1(a) and 1(b) we can see that the probabilities of pure p-shell configuration, $P(p^7)$, needed to obtain a given value of logft are rather close to each other with differences of $\leqslant 5\%$. In other words, it is rather irrelevant for the logft's whether the $\nu 1s_{1/2}$ is a halo orbit or not. Moreover, when all the single-particle energies of the sd shell, $1s_{1/2}$, $0d_{5/2}$, and $0d_{3/2}$, are lowered by the same amount as in our previous work [7] instead of lowering only the single-particle energy of the $1s_{1/2}$ orbit, the logft-P (p^7) curve remains almost unchanged. Note that, since the p-shell configuration in ^{11}Li is exhausted by the $p_{3/2}^5 p_{1/2}^2$ configuration with more than 99.9% in the present calculations, P (p^7) is actually the probability of the $\nu p_{1/2}^2$ configuration for the last two neutrons in ^{11}Li. We want to point out that the present transition rate (i.e., logft) is determined predominantly by P (p^7) and is not affected by details of the excited configurations: It is irrelevant whether two valence particles or four valence particles are excited into the sd shell.

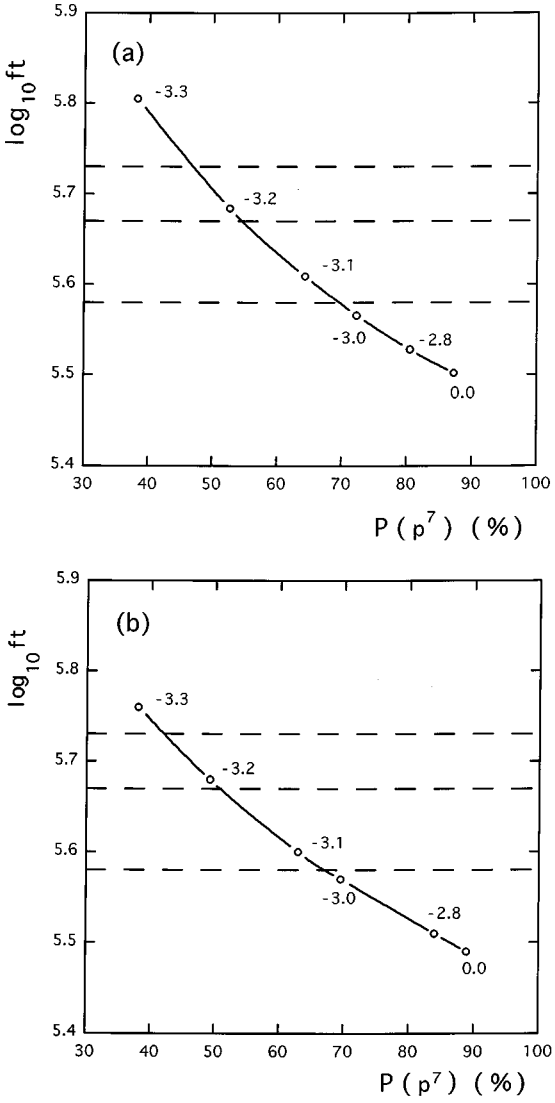

FIG. 1. Logft values of the GT transition ^{11}Li$\rightarrow^{11}$Be ($1/2^-$, 0.32 MeV) vs the probability of the pure p-shell configuration, $P(p^7)$. Dashed lines show the observed logft values: logft=5.73 ± 0.03 [9], 5.67 ± 0.04 [8], and 5.58 ± 0.03 [10]. Numbers denoted in the figure are the values of $\Delta\epsilon_{1s_{1/2}}$. (a) $\nu 1s_{1/2}$ as well as $\nu p_{1/2}$ are halo orbits. (b) Only $\nu p_{1/2}$ is a halo orbit.

The calculations fitted to the ^{11}Li ($3/2^-_{gs}$)$\rightarrow^{11}$Be ($1/2^-$,0.32 MeV) logft value measured by the three experiments are denoted hereafter as (A) for the recent ISOLDE data [9], (B) for the recent RIKEN data [8], and (C) for the old CERN data [10]. The P (p^7) turns out to be 46, 55, and 70 % in (A), (B), and (C), respectively. The single-particle energy of the $1s_{1/2}$ orbit is lowered by 3.245, 3.185, and 3.035 MeV, in (A), (B) and (C), respectively. Here, both $\nu p_{1/2}$ and $\nu 1s_{1/2}$ orbits have the halo structure. For comparison, if only $\nu p_{1/2}$ has the halo structure, the P (p^7) decreases

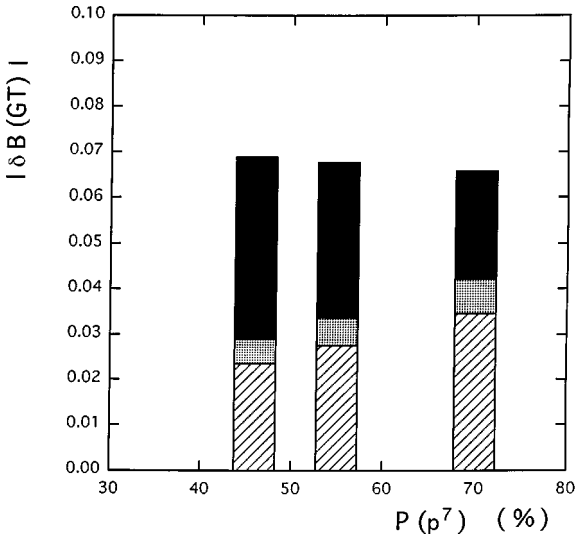

FIG. 2. The reductions of B(GT) due to the halo of $p_{1/2}$ orbit, the Δ_{33}-isobar exchange current and the admixture of the sd-shell components are denoted, respectively, by the dashed, dotted, and black histograms. The histograms correspond to fits to the three experimental data [9], [8], and [10] from left to right, respectively.

to 42, 50, and 66 %, respectively, for the three cases. If we adopt the two recent measurements, the probability of two-neutron halo in ^{11}Li is around 50%, namely, 45–55 %. Branching ratios appear to be 6.44 and 6.61 % in calculations (A) and (B), respectively. They are rather close to the observed branching ratios: 6.3 ± 0.6 % and 7.6 ± 0.8 % [8].

Figure 2 exhibits separately the variations of B(GT), denoted as δB(GT), due to the halo of the $\nu p_{1/2}$ orbit, the Δ_{33}-isobar exchange current, and the admixture of the sd-shell component. The $|\delta B(\mathrm{GT})|$ corresponding to the three different values of $P\ (p^7)$ are given. The dashed histograms show the effects of the halo of the $\nu p_{1/2}$ orbit. They decrease as $P\ (p^7)$ decreases. At first glance, the square of the overlap $\langle \pi p|\nu p_{1/2}\rangle = 0.85$ seems to indicate $\delta \log ft \sim 0.14$ if the transition is dominated by the pure $\nu p_{1/2} \rightarrow \pi p_{3/2}$ transition. However, the GT transition matrix element in the p shell consists of four components, $\nu p_{1/2} \rightarrow \pi p_{1/2}$, $\nu p_{1/2} \rightarrow \pi p_{3/2}$, $\nu p_{3/2} \rightarrow \pi p_{1/2}$, and $\nu p_{3/2} \rightarrow \pi p_{3/2}$, as shown in Table I. One finds significant cancellation among them due to the intermediate-coupling nature [13]. The halo effect due to the $\nu p_{1/2}$ orbit results in a reduction of the matrix element of the $\nu p_{1/2} \rightarrow \pi p_{3/2}$ transition by 15%. As the other three components cancel a large part of this contribution, the net reduction by the halo is magnified and the total GT matrix element is reduced by 44%. This gives rise to $\delta \log ft \sim \log 1/(0.56)^2 \sim 0.5$.

TABLE I. Matrix elements of the GT transition $^{11}\mathrm{Li} \rightarrow {}^{11}\mathrm{Be}$ ($1/2^-$,0.32 MeV) corresponding to the case (B) (Ref. [8]). Comparison is made between the results with the harmonic oscillator (h.o.) basis and the halo wave function (w.f.) for $\nu p_{1/2}$.

Neutron→	Proton	h.o. s.p. basis	halo s.p. w.f. for $p_{1/2}$
$p_{1/2}$	$p_{1/2}$	0.0022	0.0019
$p_{3/2}$	$p_{1/2}$	0.2890	0.2890
$p_{1/2}$	$p_{3/2}$	−1.3935	−1.1845
$p_{3/2}$	$p_{3/2}$	0.6225	0.6225
Sum		−0.4798	−0.2711

The dotted histograms in Fig. 2 show the contributions of the Δ_{33}-isobar exchange current. This effect is evaluated only for the p-shell part of the transition. As the $P\ (p^7)$ decreases, the contributions become somewhat smaller. The black histograms exhibit contributions of the admixture of the sd-shell components. The effects of the halo of the $\nu 1s_{1/2}$ orbit and of the Δ_{33}-isobar exchange current in the sd shell are included. They increase as $P\ (p^7)$ decreases, as we expect. The sum of the three contributions results in $\delta \log ft = 0.9 \sim 1.0$, a tremendous retardation.

B. The GT sum rule and sum of β^- transitions

We extend our study to the strength distribution of the GT transitions $^{11}\mathrm{Li}\ (3/2^-_{\mathrm{gs}}) \rightarrow {}^{11}\mathrm{Be}^*\ (1/2^-, 3/2^-, 5/2^-)$, which must exist according to the sum rule [16]: $S_{\beta^-} - S_{\beta^+} = 3(N-Z) = 15$ where $S_{\beta^-} = \Sigma_f |\langle f|\sigma t_-|i\rangle|^2$ and $S_{\beta^+} = \Sigma_f |\langle f|\sigma t_+|i\rangle|^2$. The relations $S_{\beta^-} = 15$ and $S_{\beta^+} = 0$ can be easily shown for the closed neutron p shell. If we assume a simple configuration with one proton in the $p_{3/2}$ shell and six neutrons in the $p_{3/2}$ and $p_{1/2}$ closed shells, S_{β^-} is calculated to be

$$S_{\beta^-} = |\langle p_{1/2}\|\sigma\|p_{1/2}\rangle|^2 + \tfrac{3}{4}\,|\langle p_{3/2}\|\sigma\|p_{1/2}\rangle|^2 + |\langle p_{1/2}\|\sigma\|p_{3/2}\rangle|^2 + \tfrac{3}{4}\,|\langle p_{3/2}\|\sigma\|p_{3/2}\rangle|^2 = \tfrac{2}{3} + \tfrac{3}{4}\,\tfrac{16}{3} + \tfrac{16}{3} + \tfrac{3}{4}\,\tfrac{20}{3} = 15, \tag{1}$$

and $S_{\beta^+} = 0$ since the proton in the $p_{3/2}$ shell cannot change to a neutron. The factor 3/4 in Eq. (1) represents the Pauli blocking. When the proton is in the $p_{1/2}$ shell, we obtain the same result; $S_{\beta^-} = 15$ again and $S_{\beta^+} = 0$.

When the two $p_{1/2}$ neutrons are excited into the $1s_{1/2}$ shell, $S_{\beta^-} = 49/3 > 15$ and $S_{\beta^+} = 4/3$, if we assume that one proton is in the $p_{3/2}$ shell. In this case,

$$S_{\beta^-} = \frac{3}{4}\,|\langle p_{3/2}\|\sigma\|p_{3/2}\rangle|^2 + |\langle p_{1/2}\|\sigma\|p_{3/2}\rangle|^2 + |\langle 1s_{1/2}\|\sigma\|1s_{1/2}\rangle|^2 = \frac{3}{4}\,\frac{20}{3} + \frac{16}{3} + 6 = \frac{49}{3}, \tag{2}$$

and

$$S_{\beta^+} = \frac{1}{4}\,|\langle p_{1/2}\|\sigma\|p_{3/2}\rangle|^2 = \frac{1}{4}\,\frac{16}{3} = \frac{4}{3}. \tag{3}$$

The result of Eq. (2) remains unchanged if the two $p_{1/2}$ neutrons are excited into the sd shell without restriction to the $1s_{1/2}$ orbit. The sum rule, $S_{\beta^-} - S_{\beta^+} = 15$, is satisfied. We discussed in the previous section that the two-neutron halo state of ^{11}Li is a mixture of $\nu p_{1/2}^2$ and $\nu 1s_{1/2}^2$ configurations. The GT transition $^{11}\mathrm{Li}\ (3/2^-_{\mathrm{gs}}) \rightarrow {}^{11}\mathrm{Be}\ (1/2^-, 0.32\ \mathrm{MeV})$ indicates that two neutrons forming the halo consist of the $p_{1/2}^2$ configuration with probability 45–55 %. When the two configurations are mixed with α being the probability of the $\nu p_{1/2}^2$ configuration, one ends up with $S_{\beta^-} = 15\alpha + 49/3(1-\alpha) = 49/3 - 4/3\alpha$ and $S_{\beta^+} = 4/3(1-\alpha)$. The sum rule, $S_{\beta^-} - S_{\beta^+} = 15$, remains valid.

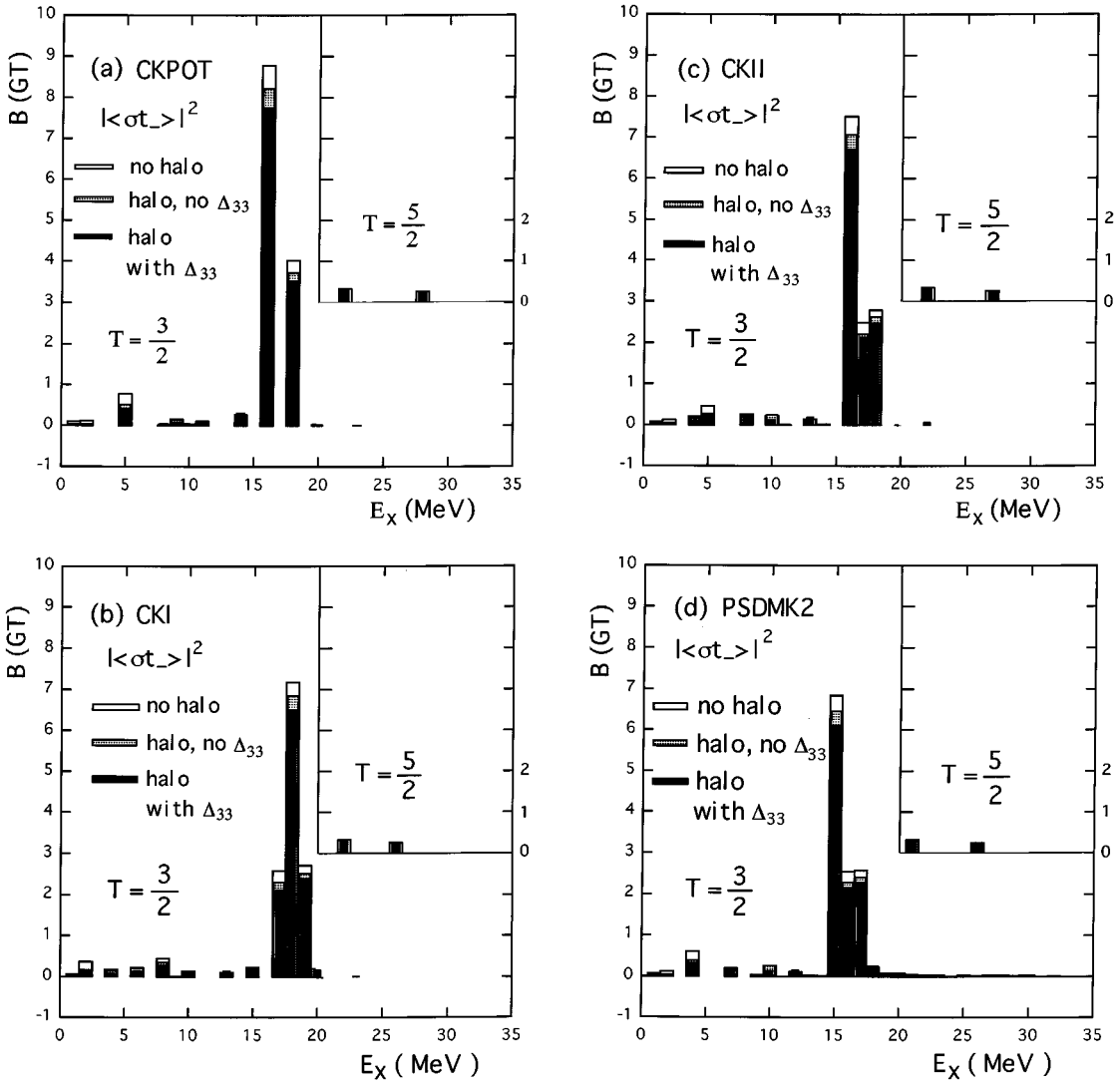

FIG. 3. Calculated GT strengths S_{β^-} for ^{11}Li $(3/2^-_{gs})\rightarrow{}^{11}$Be* $(1/2^-,3/2^-,5/2^-)$ as functions of excitation energy (E_x) of ^{11}Be. The sum of the strength within $E_x=N-0.5-N+0.5$ MeV (N=integer) is plotted. Black and dashed histograms are obtained with (without) the Δ_{33} contributions, including the halo effects. White histograms include neither the halo effects nor the Δ_{33} contributions. Wave functions obtained by using the three Cohen-Kurath interactions (denoted as CKPOT, CKI, and CKII) in the p shell and the Millener-Kurath interaction (denoted as PSDMK2) in the p-sd shell are used.

The halo reduces the overlap of radial wave functions of proton states ($\pi p_{1/2}$ and $\pi p_{3/2}$) with that of the $\nu p_{1/2}$ state, as well as the overlap of the radial wave function of $\pi 1s_{1/2}$ with that of $\nu 1s_{1/2}$. When the reductions of the overlaps due to the halo are taken into account, one obtains for the case of the excitation of the $p_{1/2}$ neutrons into the $1s_{1/2}$ shell

$$S^{\rm halo}_{\beta^-}=13.705\alpha+12.677(1-\alpha),$$

$$S^{\rm halo}_{\beta^+}=0.963(1-\alpha), \tag{4}$$

resulting in $S^{\rm halo}_{\beta^-}-S^{\rm halo}_{\beta^+}=11.714+1.991\alpha$. For $\alpha=50\%$, $S^{\rm halo}_{\beta^-}=13.191$, $S^{\rm halo}_{\beta^+}=0.482$, and $S^{\rm halo}_{\beta^-}-S^{\rm halo}_{\beta^+}=12.710$. The sum rule, $S_{\beta^-}-S_{\beta^+}=15$, is not satisfied any more. The missing strengths are outside the present p-sd model space.

Although $p_{1/2}$ neutrons are excited not only into $1s_{1/2}$ shell but also into $d_{5/2}$ and $d_{3/2}$ orbits, about 1/2–2/3 of the excited neutrons are in the $1s_{1/2}$ orbit for $P\,(p^7)$ $=70-45\,\%$. Including excitations to all sd-shell orbits, the values for $S^{\rm halo}_{\beta^-}$ in the three calculations (A), (B), and (C) are given as

$$S^{\rm halo}_{\beta^-}=13.705\alpha+14.469(1-\alpha),$$

$$S^{\rm halo}_{\beta^-}=13.705\alpha+14.034(1-\alpha),$$

$$S^{\rm halo}_{\beta^-}=13.705\alpha+13.884(1-\alpha), \tag{5}$$

and, by using the respective values of α, $S^{\rm halo}_{\beta^-}$ turns out to be 13.93, 13.85, and 13.80, respectively.

C. GT distribution in ^{11}Li

We now turn to GT transitions to higher states as in ^{11}Li $(3/2^-)\rightarrow{}^{11}$Be* $(1/2^-,3/2^-,5/2^-)$. As ^{11}Li is a neutron-rich nucleus, the potential for protons is deeper than that for neutrons and, therefore, most of the β^- decays can occur for

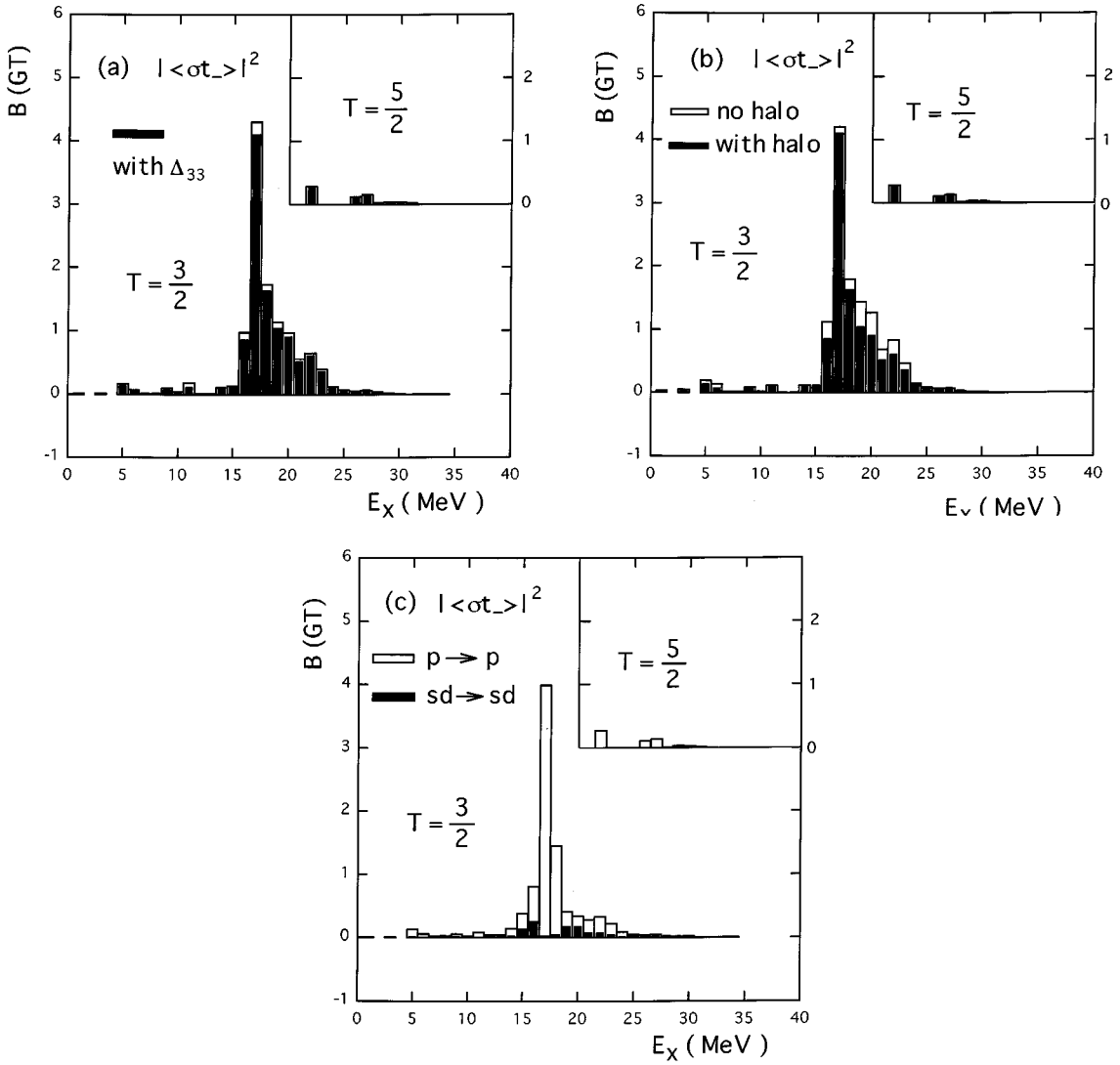

FIG. 4. (a) Calculated GT strengths S_{β^-} for ^{11}Li $(3/2^-_{gs})\rightarrow{}^{11}$Be* $(1/2^-,3/2^-,5/2^-)$ as functions of excitation energy (E_x) of ^{11}Be. The sum of the strength within $E_x=N-0.5-N+0.5$ MeV ($N=$integer) is plotted. Black (white) histograms are obtained with (without) the Δ_{33} contributions. Here, the single-particle energies of the $1s_{1/2}$ shell are lowered to increase the probability of the admixture of the $p^5(sd)^2$ configurations: $P(p^7)=46\%$. (b) Effects of the halo on S_{β^-}. The black histograms obtained with the halo effects are the same as in (a). The white ones are obtained without the halo effects. (c) The same as in (a) for separate contributions from $0p\rightarrow 0p$, and $1s\rightarrow 1s$ and $0d\rightarrow 0d$ transitions.

this nucleus. Thus a large part of the GT strength can be observed by means of β^- decay. This is characteristic for neutron-rich nuclei such as ^{11}Li and is in contrast to the case of stable nuclei.

In the following, we discuss our results for the GT strength S_{β^-} for ^{11}Li $(3/2^-_{gs})\rightarrow{}^{11}$Be $(1/2^-,3/2^-,5/2^-)$. Effects of the halo in the $\nu p_{1/2}$ and $\nu 1s_{1/2}$ orbits are taken into account. The single-particle energy of the $\nu 1s_{1/2}$ orbit is lowered to reproduce the logft value of the transition to ^{11}Be $(1/2^-,0.32$ MeV). The three cases (A), (B), and (C) introduced in Sec. II A are treated. The same interaction as in Sec. II A is used and excitations of up to two valence particles to the sd shell are included.

After a neutron is changed to a proton by the β-decay process, the rest of the neutrons are assumed to remain in their orbits, constituting a doorway state. Due to the large neutron excess in ^{11}Be, the potential for protons is deeper than that for usual stable nuclei, and even the $0d_{5/2}$ $(1s_{1/2})$ state is a bound state (almost a bound state). The tail of the $1s_{1/2}$ wave function damps quickly due to the Coulomb barrier. Thus, the proton single-particle wave function can be approximated by the harmonic oscillator one. Although for high-lying states in ^{11}Be the particles are in continuum states, we assume here that a good fraction of the excitation energy is used to excite the ^{10}Be core. This and the above doorway process leads to low branching ratios for neutron emission from high-lying ^{11}Be states to low-lying ^{10}Be states, despite the favorable phase space. These low branching ratios seem to be consistent with experiment [8].

We first show (i) S_{β^-} calculated within the p shell by the Cohen-Kurath interactions [13], and (ii) S_{β^-} obtained in the p-sd model space with the use of the Millener-Kurath interaction [15] without change of the single-particle energies of the sd shell. The calculated results obtained by the Cohen-Kurath interactions, POT (8-16), TBE (6-16), and TBE (8-16), which are denoted as CKPOT, CKI, and CKII respec-

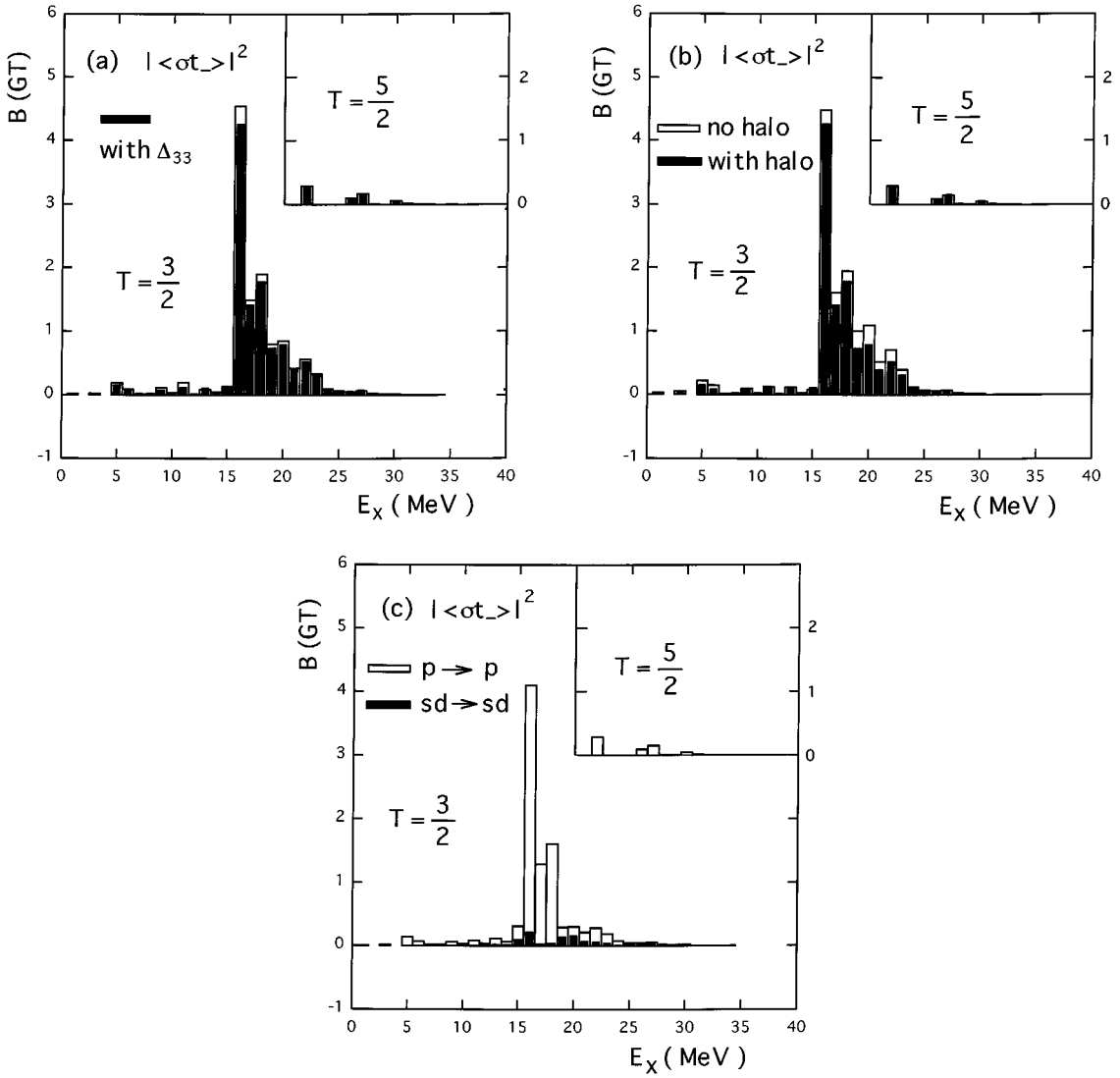

FIG. 5. The same as in Fig. 4 for the case of $P(p^7)=55\%$.

tively, are shown in Figs. 3(a)–3(c). Note that this belongs to type (i) mentioned above. Here, the partial sum of the strength for $E_x=N-0.5-N+0.5$ MeV ($N=$integer) is plotted. The calculated S_{β^-} have peaks around $E_x=16$, 18, and 16 MeV in Figs. 3(a)–3(c), respectively. Most of the GT strength is concentrated within the range of 3 MeV. Both the halo and the Δ_{33}-isobar exchange current reduce the strength. The calculated results for the p-sd model space [i.e., type (ii)], obtained by the Millener-Kurath interaction (denoted as PSDMK2), are shown in Fig. 3(d). The p-shell part of the interaction is the same as TBE (8-16) in Fig. 3(b).

The overall distribution of the strength in Fig. 3(d) is similar to the case in Fig. 3(c) except that the peak position is lowered by about 1 MeV and that the strength distribution is more spread. The small peaks of S_{β^-} in Figs. 3(a)–3(d) at $E_x\sim 22$ MeV are due to the GT transitions to the isobaric analog state (IAS), and those at $E_x=26-28$ MeV are due to the GT transitions to $T=5/2$ states.

Figures 4, 5, and 6 show S_{β^-} calculated for the cases (A), (B), and (C), respectively, as functions of the excitation energy (E_x) of ^{11}Be. Note that $\alpha=46$, 55, and 70 % in (A), (B), and (C), respectively. The single-particle energy of the $1s_{1/2}$ orbit is lowered by 3.245, 3.185, and 3.035 MeV in (A), (B), and (C), respectively.

The calculated S_{β^-} have peaks around $E_x=16-17$ MeV. We find that, as $\alpha=P$ (p^7) decreases (i.e., as moving from Fig. 6 to Fig. 5 then to Fig. 4), the main peak becomes wider and more strength emerges in the higher-energy region above the peak. The small peaks with a strength of 0.28 at $E_x\sim 22$ MeV (shown in the right upper part of the graphs) correspond to the transition to the IAS. The small peaks with a strength of 0.14–0.15 at $E_x\sim 27$ MeV are contributions due to $T=5/2$ states. The S_{β^-} summed up to the IAS energy ($E_{\rm IAS}$) turn out to be 10.22 (11.05), 10.58 (11.41), and 11.13 (11.97) for the calculations (A), (B), and (C), respectively, for the case with (without) the Δ_{33} contributions. A quenching of the strength by 7–8 % due to the coupling to the Δ-hole configurations is seen. The total S_{β^-} expected in the present p-sd shell calculation is 13.44, 13.63, and 13.81, respectively, for the three cases without the Δ_{33} contributions. About 2/3 of the sum rule value can be observed by β^- decay. The missing part of the strength is expected to lie above $E_x=E_{\rm IAS}$ as is displayed in Figs. 4(a), 5(a), and 6(a).

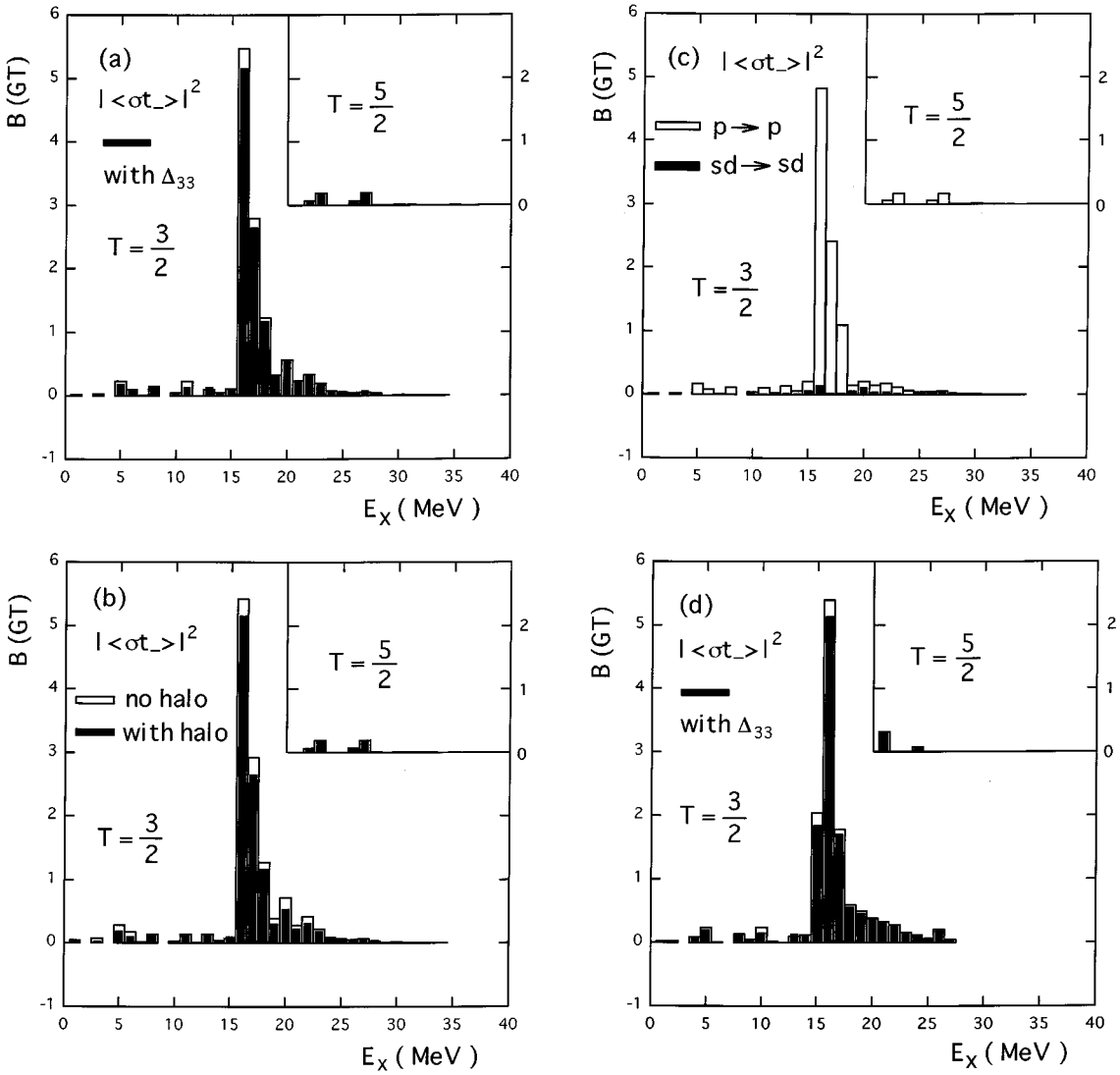

FIG. 6. The same as in Fig. 4 for the case of $P(p^7)=70\%$.

As there are many states in ^{11}Be up to $E_x=E_{\rm IAS}$, the GT strength for the decay of ^{11}Li has a resonancelike pattern, and the peak can be called a GT giant resonance. This is also a characteristic and unique point for ^{11}Li, since this pattern cannot be seen in other neighboring stable nuclei. There, the GT strength is fragmented among only a few levels and there is no resonancelike peak.

We show in Figs. 4(b), 5(b), and 6(b) how the halo affects S_{β^-}. The Δ_{33} contributions are included. The S_{β^-} summed up to $E_x=E_{\rm IAS}$ are 12.01, 12.22, and 12.48, respectively, for the three cases without the halo effects. The halo reduces S_{β^-} by 1.79, 1.64, and 1.35, respectively. On the other hand, the Δ_{33} reduces S_{β^-} by 0.83∼0.84. The reduction by the halo is caused mainly by the reduction of the overlap of the $\nu p_{1/2}$ halo wave function with the $\pi p_{3/2,1/2}$ wave functions.

We decompose S_{β^-} into contributions due to $0p\rightarrow 0p$ transitions and those due to $1s\rightarrow 1s$ and $0d\rightarrow 0d$ transitions. The calculated S_{β^-} are shown in Figs. 4(c), 5(c), and 6(c). Note that the additive sum of the two contributions is not equal to the total S_{β^-}, since there are interferences between them. We can see from the figures that, although the main contributions are attributed to the $0p\rightarrow 0p$ transitions, there are also non-negligible contributions from $1s\rightarrow 1s$ and $0d\rightarrow 0d$ transitions at energies around the peak at E_x ∼16 MeV. We also find some strength from $1s\rightarrow 1s$ and $0d\rightarrow 0d$ contributions at E_x∼20 MeV, which gives rise to the strength in the higher-energy region beyond the peak position.

We compare these calculated strengths to the case in which all the sd-shell single-particle energies are lowered by an equal amount. Figure 6(d) shows the calculated S_{β^-} for the case of $\Delta\epsilon_s=\Delta\epsilon_d=-2.2$ MeV. Here, $P(p^7)=62\%$, and the logft value for the transition to ^{11}Be ($1/2^-$, 0.32 MeV) corresponds to the measurement by Roeckl *et al.* [10] [i.e., case (C)]. Comparing Figs. 6(a) to 6(d), we find that the difference in the GT distributions is rather small.

Next, we compare the strengths shown in Figs. 4–6, to the case without lowering of the single-particle energies of the sd shell. In this case, the probability of the $\nu p_{1/2}^2$ configuration of ^{11}Li is $\alpha=89\%$ [7]. The calculated results have already been shown in Fig. 3(d). Although the position of the peak of the strength is shifted only slightly, the distribution of the strength differs to a larger extent from those in Figs. 4(a), 5(a), and 6(a). The calculated summed strength below $E_x=E_{\rm IAS}=21.5$ MeV amounts to 11.90 (12.68) for the case

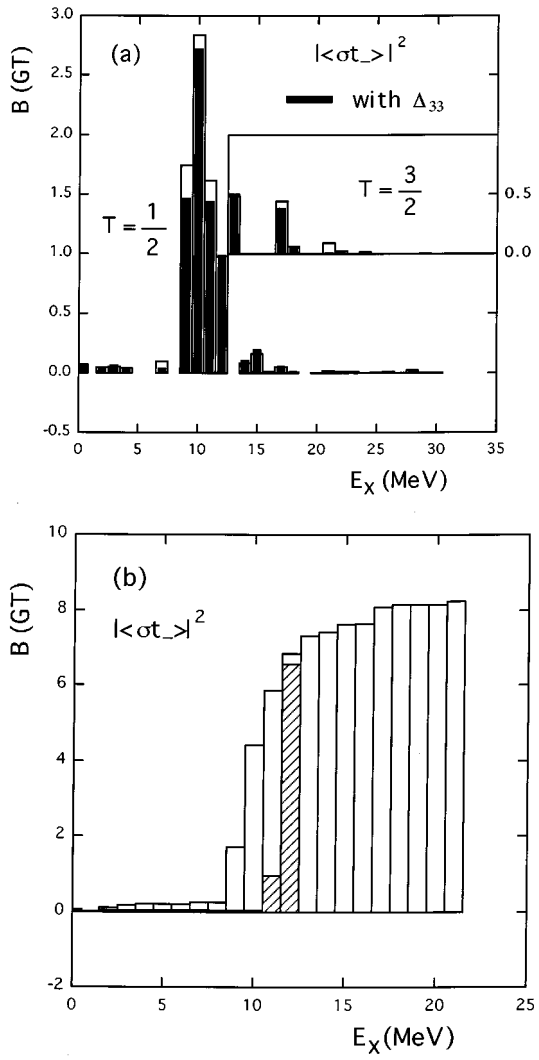

FIG. 7. (a) Calculated GT strength S_{β^-} for ^{9}Li $(3/2^-_{gs})\rightarrow{}^9$Be $(1/2^-,3/2^-,5/2^-)$. Black (white) histograms are obtained with (without) the Δ_{33} contributions. (b) Sum of GT strength up to the excitation energy (E_x) of ^{9}Be for GT transitions in ^{9}Li $(3/2^-_{gs})\rightarrow{}^9$Be $(1/2^-,3/2^-,5/2^-)$. White (dashed) histograms correspond to calculation (experiment [19]). Experimental data are taken up to $E_x=11.81$ MeV.

with (without) the Δ_{33} contributions, while the total strength in the present p-sd space is 13.84 for $\alpha=0.89$. Here, the structure of the strength distribution is much simpler than for the case with $\Delta\epsilon_{1s_{1/2}}\neq 0$. Almost all the strength below $E_x=21.5$ MeV comes from the contributions of $0p\rightarrow 0p$ transitions. The strength due to $0p\rightarrow 0p$ transitions is quite reduced above $E_x=E_{\rm IAS}$. The strength due to $1s\rightarrow 1s$ and $0d\rightarrow 0d$ transitions is completely separated from the $0p\rightarrow 0p$ ones, and resides much beyond $E_x=E_{\rm IAS}$.

Comparing the cases with and without the modification of the shell gap, we notice the following: When the single-particle energies of the sd shell are lowered, not only the $0p\rightarrow 0p$, but also the $1s\rightarrow 1s$ and $0d\rightarrow 0d$ transitions show up in the lower-energy region, resulting in a sizable strength above the main peak below the IAS. If the single-particle energies of the sd shell are not changed, the strength due to $1s\rightarrow 1s$ and $0d\rightarrow 0d$ transitions is not found below $E_x=E_{\rm IAS}$.

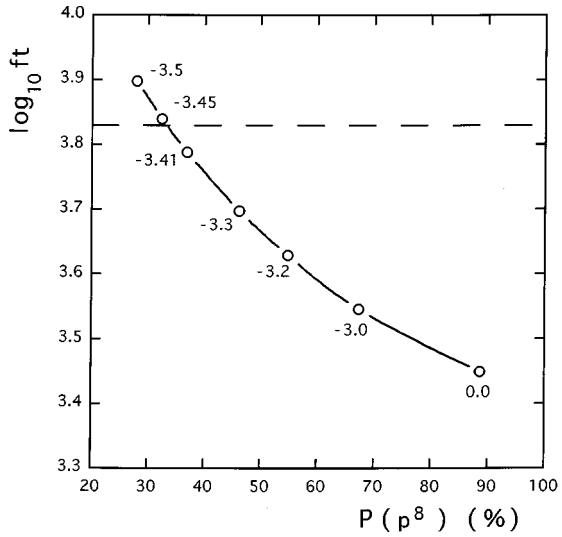

FIG. 8. Logft values of the GT transition ^{12}Be$\rightarrow{}^{12}$B (1^+_{gs}) vs the probability of the pure p-shell configurations, $P(p^8)$. Numbers denoted in the figure are values of $\Delta\epsilon_{1s_{1/2}}$. The dashed line shows the observed logft value [11].

The structure of the strength is clearly different between the two cases, $\Delta\epsilon_{1s_{1/2}}=0$ and $\Delta\epsilon_{1s_{1/2}}\neq 0$. It would be quite interesting if we could distinguish the two cases by experiment. The measurement of the magnitude of the strength would also be quite interesting to clarify the effects of quenching and spreading of the GT strength. There is a preliminary report [17,9] that substantial GT strength has been found around $E_x=18.5$ MeV.

We now comment on the dependence of S_{β^-} on the two-body interactions. When the interaction of Warburton and Brown (WBT) [18] is used, the position of the peak appears around $E_x=13$ MeV. This value is lower by 3 MeV than that obtained by the Millener-Kurath interaction, and is too low compared to the experimental one [17,9]. The WBT interaction leads to more strength at the lower-energy side compared with the Millener-Kurath interaction. The WBT interaction gives 16 states with $J^p=1/2^-$, $3/2^-$ or $5/2^-$ below $E_x=8$ MeV, while the Millener-Kurath interaction gives 11 states. The latter is close to observed number of levels below $E_x=8.05$ MeV, that is, 8–9 states [8]. The Millener-Kurath interaction adopted here reproduces rather well the peak position of the strength as well as the logft values of transitions to several low-lying states. Preliminary experimental values are reported [8] as log$ft=4.87\pm 0.08$ at $E_x=2.69$ MeV and log$ft=4.43\pm 0.08$ at $E_x=8.05\pm 0.05$ MeV. The calculated logft values obtained by the Millener-Kurath interaction are 4.73 and 4.56, respectively, for case (B). They are remarkably close to the observed ones.

III. GT TRANSITIONS IN ^{9}Li

Here, we study GT transitions in neighboring stable nuclei: ^{9}Li $(3/2^-)\rightarrow{}^9$Be$(1/2^-,3/2^-,5/2^-)$. A recent experimental investigation [19] indicates a strong feeding to the 11.81 MeV state in ^{9}Be with logft value of 2.84. The deduced GT strength is 5.6 ± 1.2. Total sum of S_{β^-} observed up to this energy ($E_x=11.81$ MeV) is 6.56, which is about 2/3 of the sum rule; $S_{\beta^-}-S_{\beta^+}=9$.

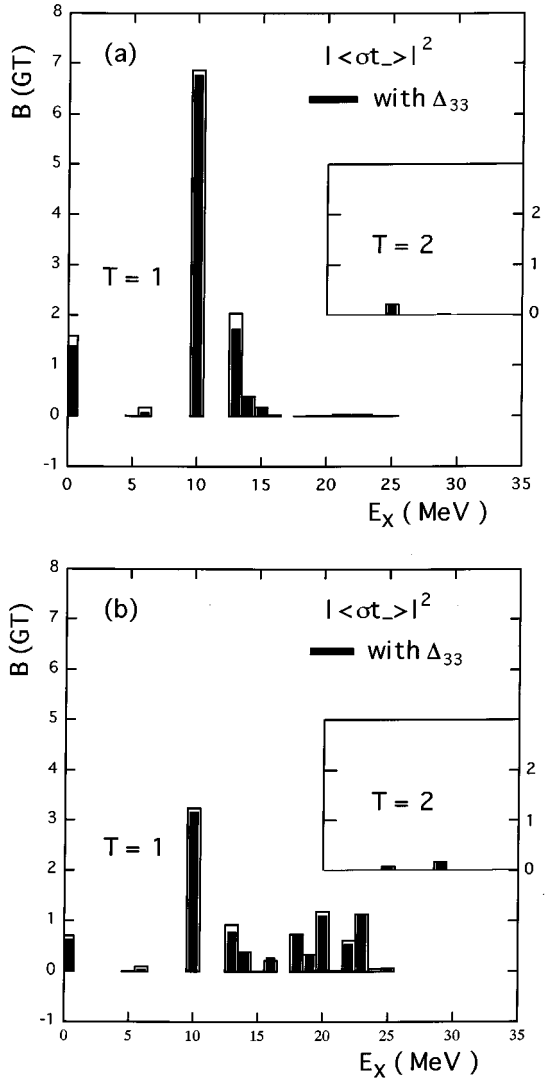

FIG. 9. Calculated GT strength S_{β^-} for ^{12}Be$\rightarrow^{12}$B (1^+). Black (white) histograms are obtained with (without) the Δ_{33} contributions. $\Delta\epsilon_{1s_{1/2}}$ is equal to (a) 0.0 MeV and (b) -3.41 MeV, respectively. The left most parts of the histograms ($0 \leqslant E_x \leqslant 0.5$ MeV) actually correspond to the transition to the ground state ($E_x = 0.0$ MeV).

Figure 7(a) shows the calculated GT strength, S_{β^-}, for each energy bin, and Fig. 7(b) exhibits the sum of the strength up to a certain excitation energy of ^{9}Be. Similar to the ^{11}Li case, the p-sd shell-model configuration space is used with the Millener-Kurath interaction. The single-particle energies of the sd shell are not changed. As shown in Fig. 7(a), S_{β^-} has a peak around $E_x = 10$ MeV. S_{β^-} up to $E_x = 13.5$ MeV is 6.85 (7.48) with (without) the Δ_{33} contributions. This value of 6.85 for S_{β^-} agrees well with the experimental one, which is 6.56 [19]. Most of the strength is distributed near the peak region; $S_{\beta^-} = 5.62$ (6.19) in the energy region $E_x = 8.5$–11.5 MeV with (without) the Δ_{33} contributions. According to a recent observation [19], this amount of strength, 5.6 ± 1.2, is concentrated in one state at $E_x = 11.81$ MeV.

The calculated and observed sums S_{β^-} are given in Fig. 7(b). A rather good agreement between experiment and calculation is obtained around the energy region $E_x \sim 12$ MeV where most of the observed strength is found, though there remain some discrepancies at low excitation energies with tiny GT strength. The discrepancy between the calculation and experiment at $E_x = 9-11$ MeV reflects the fact that most of the observed strength is concentrated in one state at $E_x = 11.81$ MeV as stated above. It will be of interest to confirm experimentally the GT strength distributions in this energy region. The comparison between experimental and calculated GT distributions for the β decay of ^{9}Li indicates an overall agreement. It is seen also that the peak position can be predicted by the Cohen-Kurath interaction within a few (~ 2 MeV) MeV. This observation suggests that the actual peak of the GT strength distribution from ^{11}Li is located most likely within a few MeV (~ 2 MeV) around the present prediction of $E_x \sim 16$ MeV.

IV. GT TRANSITIONS IN ^{12}BE AND THE STRUCTURE OF ^{12}BE

Here, we investigate GT transitions in ^{12}Be, a neighboring isotone of ^{11}Li. We study effects due to the narrowing of the gap between p and sd shells in ^{12}Be as in the case of ^{11}Li. The experimental logft value of the GT transition $^{12}\text{Be}\rightarrow^{12}\text{Be}\ (1^+_{\text{gs}})$ is 3.834 ± 0.017 [11], which is large compared to the standard shell-model predictions within the p shell. The Cohen-Kurath interactions TBE (8-16), TBE (6-16), and POT (8-16) give, however, much smaller logft values of 3.48, 3.39, and 3.53, respectively, including the Δ_{33}-isobar exchange current corrections.

Now, in order to explain this difference (δ log$ft \sim 0.4$), we increase the probability of the $p^6(sd)^2$ configurations by lowering the single-particle energy of the $1s_{1/2}$ orbit in the p-sd shell-model calculations. We use the same interaction as in Secs. II and III, allowing excitation of two valence particles into the sd shell. The calculated results are shown in Fig. 8 as a function of the probability of the pure p-shell configurations, P (p^8). The values of $\Delta\epsilon_{1s_{1/2}}$ are denoted in the figure. We need about 65% breaking of the neutron p-shell closure in order to reproduce the experimental logft value. This result suggests a tremendous breaking of the core of ^{12}Be. It is practically irrelevant whether two valence particles or four valence particles are excited into the sd shell.

A similar result was noticed from simpler estimates in Refs. [20] and [21]. In Ref. [20], the ground state of ^{12}Be is treated as a simple $^{10}\text{Be}(0^+) + 2\nu$ state with the two neutrons in $p^2_{1/2}$, $d^2_{5/2}$, or $1s^2_{1/2}$ configurations with single-particle energies for the spherical ^{10}Be core adjusted so that ^{11}Be spectrum is reproduced. The reduction factor of the $p^2_{1/2}$ configuration obtained in Ref. [20] was then used in Ref. [21] to estimate the retardation of the GT transition from ^{12}Be and compare with the observation of the lifetime. They suggested a large ($\sim 60\%$) breaking of the p-shell closure in ^{12}Be.

Next, we show the calculated GT distributions of ^{12}Be for the case with and without the lowering of the single-particle energy of the $1s_{1/2}$ orbit. The calculated results with $\Delta\epsilon_{1s_{1/2}} = 0.0$ MeV are shown in Fig. 9(a). The strength is distributed among 3–4 bunches. The strength at $E_x \sim 25$ MeV is due to the contribution from the transition to the IAS. Results with $\Delta\epsilon_{1s_{1/2}} = -3.41$ MeV are shown in Fig. 9(b). This corresponds to the case where the logft value of

the transition to ^{12}B (1^+_{gs}) reproduces the observed value: $\log ft = 3.8$ [11]. The calculated strength at $E_x \sim 0$ and 10 MeV is quenched by about 50%. The strength is distributed among several bunches and is more concentrated in the higher-energy region. Small peaks at $E_x \sim 25$ and 29 MeV are contributions to the $T=2$ states. We see a clear difference between the two cases $\Delta\epsilon_{1s_{1/2}} < 0$ and $\Delta\epsilon_{1s_{1/2}} = 0$. It would be extremely interesting to measure the GT strength distribution in ^{12}Be.

V. SUMMARY

In summary, the β decay of ^{9,11}Li has been studied in terms of shell-model calculations, allowing $2p$-$2h$ excitations into the sd shell. Reasonable agreement with experimental data, though preliminary in some cases, has been obtained. Note that it is not essential whether two valence particles or four or more valence particles are excited into the sd shell. The probability of $\nu p^2_{1/2}$ configurations in ^{11}Li has been reinvestigated by using the measurements at RIKEN [8] and ISOLDE [9]. The experiments indicate $P\ (p^2_{1/2}) \approx 45-55$ %, which reproduces the branching ratio also.

The GT distribution in ^{11}Li has been investigated. Effects of the halo structure and the narrowing of the p-sd shell gap are seen in the B(GT) peak position and distribution pattern. As the single-particle energy of the $1s_{1/2}$ orbit is lowered, the GT distribution becomes more fragmented: the height of the GT peak becomes lower, its width gets larger, and more strength is found in the higher-energy region. About 2/3 of the sum rule value of the strength is found below $E_x = E_{\rm IAS}$, which can be observed by β^- decay. GT transitions in ^{12}Be has also been studied. A tremendous breaking of the p-shell core of ^{12}Be is suggested.

ACKNOWLEDGMENTS

The authors would like to express their thanks to S. Shimoura, N. Aoi, and K. Riisager for informing them of their experimental results prior to publication. They also thank W. Bentz for careful reading of the manuscript. This work was supported in part by Grant-in-Aids for Scientific Research on General Areas (No. 08640390) and Priority Areas (No. 05243102) from the Ministry of Education, Science, and Culture.

[1] I. Tanihata, J. Phys. G **22**, 157 (1996).
[2] P. G. Hansen, A. S. Jensen, and B. Jonson, Annu. Rev. Nucl. Part. Sci. **45**, 591 (1995).
[3] T. Kobayashi, in *Proceedings of the International Symposium on Structure and Reactions of Unstable Nuclei*, Niigata, 1991, edited by K. Ikeda and Y. Suzuki (World Scientific, Singapore, 1991), p. 187.
[4] B. M. Young *et al.*, Phys. Rev. Lett. **71**, 4124 (1993).
[5] M. Fukuda *et al.*, Phys. Lett. B **268**, 339 (1991).
[6] T. Otsuka, N. Fukunishi, and H. Sagawa, Phys. Rev. Lett. **70**, 1385 (1993).
[7] T. Suzuki and T. Otsuka, Phys. Rev. C **50**, R555 (1994).
[8] N. Aoi *et al.*, Nucl. Phys. **A616**, 181c (1997); Z. Phys. A (to be published).
[9] M. J. G. Borge *et al.*, Phys. Rev. C **55**, R8 (1997); and K. Riisager (private communication); I. Mukha *et al.*, contribution to *The Fourth International Conference on Radioactive Nuclear Beams* (RNB4), Ohmiya, Japan, 1996.
[10] E. Roeckl, D. F. Dittner, C. Détraz, R. Klapisch, C. Thibault, and C. Rigaud, Phys. Rev. C **10**, 1181 (1974).
[11] F. Ajzenberg-Selove, Nucl. Phys. **A433**, 1 (1985); **A506**, 1 (1990).
[12] OXBASH, The Oxford, Buenos-Aires, Michigan State, Shell Model Program, B. A. Brown, A. Etchegoyen, and W. D. M. Rae, MSU Cyclotron Laboratory Report No. 524, 1986.
[13] S. Cohen and D. Kurath, Nucl. Phys. **73**, 1 (1965).
[14] T. T. S. Kuo, Nucl. Phys. **A103**, 71 (1967).
[15] D. J. Millener and D. Kurath, Nucl. Phys. **A255**, 315 (1975).
[16] K. Ikeda, S. Fujii, and J. I. Fujita, Phys. Lett. **3**, 271 (1963).
[17] S. Shimoura (private communication).
[18] E. K. Warburton and B. A. Brown, Phys. Rev. C **46**, 923 (1992).
[19] G. Nyman *et al.*, Nucl. Phys. **A510**, 189 (1990).
[20] F. C. Barker, J. Phys. G **2**, L45 (1976).
[21] D. E. Alburger, D. P. Balamuth, J. M. Lind, L. Mulligan, K. C. Young, Jr., R. W. Zurmühle, and R. Middleton, Phys. Rev. C **17**, 1525 (1978).